ELSEVIER

Journal of Physics and Chemistry of Solids 62 (2001) 503–511

JOURNAL OF PHYSICS AND CHEMISTRY OF SOLIDS

www.elsevier.nl/locate/jpcs

Transition assignments to $L\beta_2$ satellites in X-ray emission spectra of higher Z elements

S. Poonia[a,*], S.N. Soni[b]

[a]*Division-I, Central Arid Zone Research Institute, Jodhpur 342003, India*
[b]*X-ray Laboratory, Physics Department, Jai Narain Vyas University, Jodhpur 342005, India*

Received 2 February 2000; accepted 19 May 2000

Abstract

The satellite spectra arising due to L_3M_x–$M_xN_{4,5}$ ($x = 1$–5) transition array in X-ray emission spectra of $_{74}$W, $_{76}$Os, $_{78}$Pt, $_{80}$Hg, $_{82}$Pb, $_{88}$Ra and $_{90}$Th, have been calculated using available HFS data on K–LM and L–MN Auger transition energies. The agreement between the calculated and measured energies, that between calculated and measured separations in energies and the consideration of the relative probabilities of all the L_3M_x–$M_xN_{4,5}$ transitions have been used as the basis for deciding the origin of the satellites. It has been established that two satellites observed in the $L\beta_2$ region of the X-ray spectra of various elements and named β_2^{I} and β_2^{II} in order of increasing energy are mainly emitted by $L_3M_{4,5}$–$M_{4,5}N_{4,5}$ transitions. It is observed that the satellite β_2^{I} in the spectra of elements with $Z = 74$–76 has been assigned to the superposition of $^3F_4$–$^3G_5$ and $^3F_4$–$^3D_3$ transitions and that it must be the most intense of all these satellites. The same transitions have been proved to be the main origin of the satellite, β_2^{II}, reported in the range $Z = 78$–90. Further, the satellite β_2^{I}, reported in the spectra of elements with $Z = {}_{74}$W to $_{76}$Os, has been associated with the transitions $^3D_3$–$^3F_4$ and $^1D_2$–$^1F_3$. Finally, the line β_2^{II}, reported in the spectra of elements $Z =$ 74–76, has been assigned to the $^1F_3$–$^1G_4$ transition. The possible contributions of other transitions of the L_3M_x–$M_xN_{4,5}$ ($x =$ 1–5) array having intensities comparable with the above transitions, and the corresponding lines, which have not yet been observed, have also been discussed.

1. Introduction

On the high-energy side of and close to the $L\beta_2$ line in the X-ray emission spectra of various elements, many weak lines have been observed. The complete data have been compiled by Cauchois and Senemaud [1] and have been graphically presented by Soni and Massoud [2]. In the spectra of elements $Z = 40$–50, five lines, named $\beta_2^{(a)}$, β_2^{I}, $\beta_2^{(b)}$, β_2^{II} and $\beta_2^{(c)}$ in the order of increasing energy have been reported [1]. The measured data on satellites in this region of the emission spectra of elements with $Z = 51$–71 are very scarce while those in the spectra of elements $_{73}$Ta to $_{92}$U have been named β_2^{0}, β_2^{I}, β_2^{II}, β_2^{III}, etc. in order of increasing energy. In an earlier paper [2] it has been shown that the lines named $\beta_2^{(a)}$ ($Z < 60$) and β_2^{0} ($Z > 70$) are emitted by the superposition of all the intense L_3–$N_{4,5}$ transitions taking place in the atom when an additional ionisation in the N shell is present, and in Ref. [3] we report that the transition assignments to the satellites β_2^{I}, $\beta_2^{(b)}$, β_2^{II} and $\beta_2^{(c)}$ reported in the spectra of elements with $Z = 42$–50 are emitted by the superposition of all the intense L_3–$N_{4,5}$ transitions in presence of an M-shell spectator vacancy. In the present paper, we report the result of our calculations on the transition assignments to the one or two satellites β_2^{I} and β_2^{II} reported in the spectra of elements with $Z = 74$–90. The proper candidates, thought of in the present study, are L_3–$N_{4,5}$ transitions in the presence of an M-shell spectator vacancy. It is well established that intermediate coupling is most suitable for the middle Z elements, while j–j coupling should be applied for elements near the end of the periodic table.

* Corresponding author. Tel.: +91-291-740-534; fax: +91-291-740-706.

E-mail address: kundan@cazri.raj.nic.in (S. Poonia).

0022-3697/01/$ - see front matter
PII: S0022-3697(00)00198-0

2. Calculation

We have undertaken the studies of all those transitions of L_3M_x–$M_xN_{4,5}$ ($x = 1$–5) array which are allowed according to selection rules [4] $\Delta L = 0, \pm 1$, $\Delta S = 0$ and $\Delta J = 0, \pm 1$. We have calculated their HFS energies and their relative probabilities. We have computed the spectra arising out of the superposition of these transitions in the spectra of an element by assuming each transition to give rise to a Gaussian line. Finally, these computed spectra have been compared with the observed satellite spectra [2].

2.1. The transition energies

The energies of the transition, used in the present study, have been calculated by the combination formula:

$$E(L_3M_x\text{–}M_xN_{4,5}) = E(K\alpha_1) - E(K\text{–}L_3M_x) + E(L_3\text{–}M_xN_{4,5}) \quad (1)$$

where $E(K\alpha_1)$ is the energy of the $K\alpha_1$ line. Its value has been taken from the tables of Bearden and Burr [5]. E(K–LM) and $E(L_3$–MN) are the Auger electron energies for the K–LM and L_3–MN transitions, respectively. These energies have been taken from the tables of Larkins [6], who has calculated various two-hole state energies of atoms with $Z = 10$–100 in the intermediate coupling approximation and also has corrected them for adiabatic relaxation of the orbitals due to a sudden creation of an inner hole as well as for the solid state of the sample. His values are in good agreement with the available experimental Auger electron energy data in the region of Z values presently under study, as claimed by Larkins [6].

2.2. The transition probabilities

For the emission of $L\beta_2$ satellites in hand, those transitions are being considered in which the initial states are doubly ionised, one vacancy lying in the $2p_{3/2}$ subshell and the other in the M subshell. Such states are formed by two processes.

(1) L_1–L_3M Coster Kronig Transitions, namely conversion of one-hole state L_1 to a two-hole state L_3M_x ($x =$ 1–5) through the Auger transition L_1–L_3M_x.
(2) By the shake-off method, namely an electron from the M shell of the atom may escape out simultaneous to the formation of a $2p_{3/2}$ vacancy. This additional vacancy is created due to shaking of the atomic orbits caused by a sudden change in the potential field in the atom, taking place when a $2p_{3/2}$ electron leaves the atom with a high speed.

The Coster Kronig transition probability can be written as $\sigma\sigma'$, where σ denotes the probability of formation of a vacancy in the $2s_{1/2}$ subshell of the atom and σ' is the probability of its decay through the Coster Kronig transition L_1–L_3M. Factor σ has been calculated by the formulas given by Moores et al. [7], namely

$$\sigma_{nl} = (\pi n^4 a_0^2 Z_{nl}/Z^4)\sigma_{nl}(R) \quad (2)$$

$$\sigma_{nl} = (1.628 \times 10^{-14}) Z_{nl}\sigma_{nl}(R)/E_{nl}^2 \quad (3)$$

In these formulas n and l denote the subshell of the atom in which a hole is created, Z_{nl} denotes the total number of electrons in this subshell and E_{nl} denotes the binding energy of the electron in it. $\sigma_{nl}(R)$ is known as the reduced cross-section, and is calculated by the formula [7]

$$\sigma_{nl}(R) = (1/u)[A \ln u + B(1 - 1/u)^2 + (C/u + D/u^2)(1 - 1/u)] \quad (4)$$

These formulas have been theoretically derived by Moores et al. [7] and are applicable to single ionisation of atoms in the inner shell by electron bombardment. A, B, C and D are constants whose values for ionisation in the $2s_{1/2}$ subshell are $A = 0.823$, $B = 3.69$, $C = 0.62$, $D = 1.79$ and in the $2p_{3/2}$ subshell are $A = 0.530$, $B = 5.07$, $C = 1.20$ and $D = 2.50$ [7]. The dimensionless parameter u denotes the ratio:

$u = E_0/E_{nl}$ = Incident energy of incoming electron/B.E. of the nl electron.

Since different people who have measured the satellite spectra of various elements experimentally have used different excitation energies, we have arbitrarily taken the value of u as 2.5.

The value of $\sigma(L_1)$ so calculated has been multiplied with Coster Kronig transition probability σ', taken from table of McGuire [8]. It should be noted that the CK transitions help in forming only $L_3M_{4,5}$ stated, and that too only in the elements up to $Z = 47$ [8] and $Z = 74$–90 [8]. The other L_1–L_3M_x transitions are not allowed energetically in these elements. Further, no such CK transitions take place in elements with $Z = 48$–73 [8].

Coming to the shake-off process, we have first calculated the cross-section $\sigma(L_3)$ by formulas (2)–(4) and have then multiplied it with the shake-off probability of an M-subshell electron. This probability has been calculated by interpolation from the percentage probabilities of shake-off processes occurring with a single photoionisation in inert gases [9].

Subsequently, the total probability of creation of an initial state L_3M_x has been determined by adding both these cross-sections, calculated above.

The cross-section for a set of L_3M_x levels, with x taking any value from 1 to 5, so calculated has been assumed as the total probability of all the transitions from this set. This has been distributed statistically among all the allowed transitions from this set of levels, considering all the multiplets of the supermultiplet from various $^{(2S+1)}$(L) levels of the set and then using tables of White and Eliason for relative probabilities of the transitions of each multiplet [4]. The details of

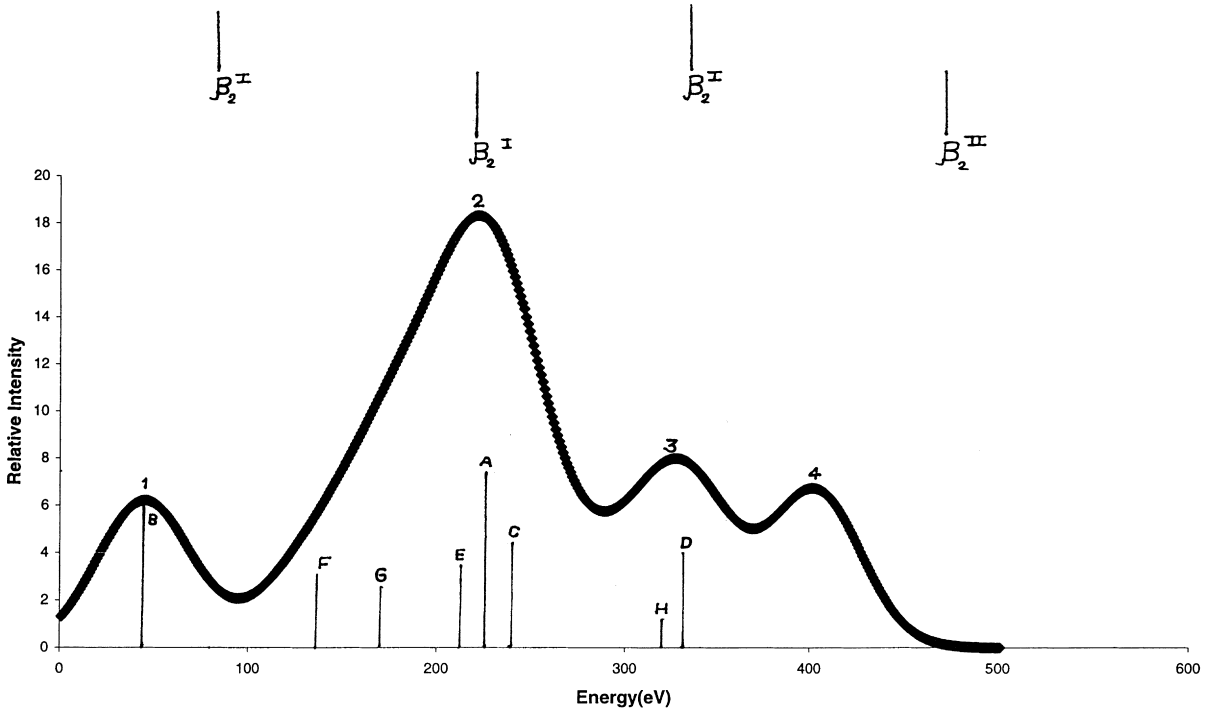

Fig. 1. The computed $L_3M–MN_{4,5}$ spectrum of $_{74}W$. The measured $L\beta_2$ satellites are shown in two rows at the top. The upper row bars are marked at energies taken from Ref. [4]. In the lower row, these are marked after adjusting the zero so that agreement between measured satellites and peaks becomes obvious.

this method have been presented in earlier papers [2,3,10,11].

2.3. Synthesis of the spectrum

We have calculated energies and intensities of all the possible transitions of the $L_3M_x–M_xN_{4,5}$ array as mentioned above. The transitions having intensity less than one-tenth of the maximum intensity of all transitions have been ignored. A composite spectrum formed by spectral lines emitted by these transitions has been computed by taking each as a Gaussian line. The choice of a Gaussian shape has been favoured over the Lorentzian one as it is more suitable for satellite spectra, as discussed by Maskil and Deutsch [12]. For this, we have taken energy on the *X*-axis and intensity on the *Y*-axis. The peak height of each line is taken equal to the transition probability and the peak position on the *X*-axis is taken at the energy of the transition. The widths of all the lines in one element have been assumed equal and this value has been decided by trial and error in such a way that the number of peaks obtained from the calculated spectrum is at least equal to or greater than the number of satellites observed experimentally in the spectrum of the element. The calculated spectra of elements with $Z = {}_{74}W$, ${}_{76}Os$, ${}_{78}Pt$, ${}_{80}Hg$, ${}_{82}Pb$, ${}_{88}Ra$ and ${}_{90}Th$ thus obtained are shown in Figs. 1–7. In these spectra, peaks of higher intensities have been recognised as the observed satellites. For the one-to-one correspondence between peaks and measured satellites, the relative energy separations of peaks and those of measured satellites have also been taken into consideration.

3. Results

Out of all the 41 transitions of $L_3M_x–M_xN_{4,5}$ ($x = 0, 1, 2$) array, 14 belonging to the $x = 3$ group have intensities that warrant attention. These are presented in Table 1, in order of decreasing intensity and the first eight are named A–H. All these transitions in the element $_{74}W$ have energies and intensities such that a superposition of corresponding Gaussian lines gives rise to a spectrum consisting of four peaks, the number increasing with rise in *Z* and becoming five in $_{90}Th$ (Figs. 1–7). A comparison of the computed spectrum of an element with the measured satellite spectrum reveals that whereas the measured satellite energies are close to those of intense peaks, their separations in the computed and measured spectra are in good mutual agreement. However, there is a systematic disagreement between the measured and calculated spectra. All the measured satellite energies in $_{74}W$ are 10–15 eV lower than the calculated peak energies. This kind of discrepancy is observed in all the presently calculated spectra, and the amount of discrepancy shows a similar, systematic and a regular variation with *Z*, as

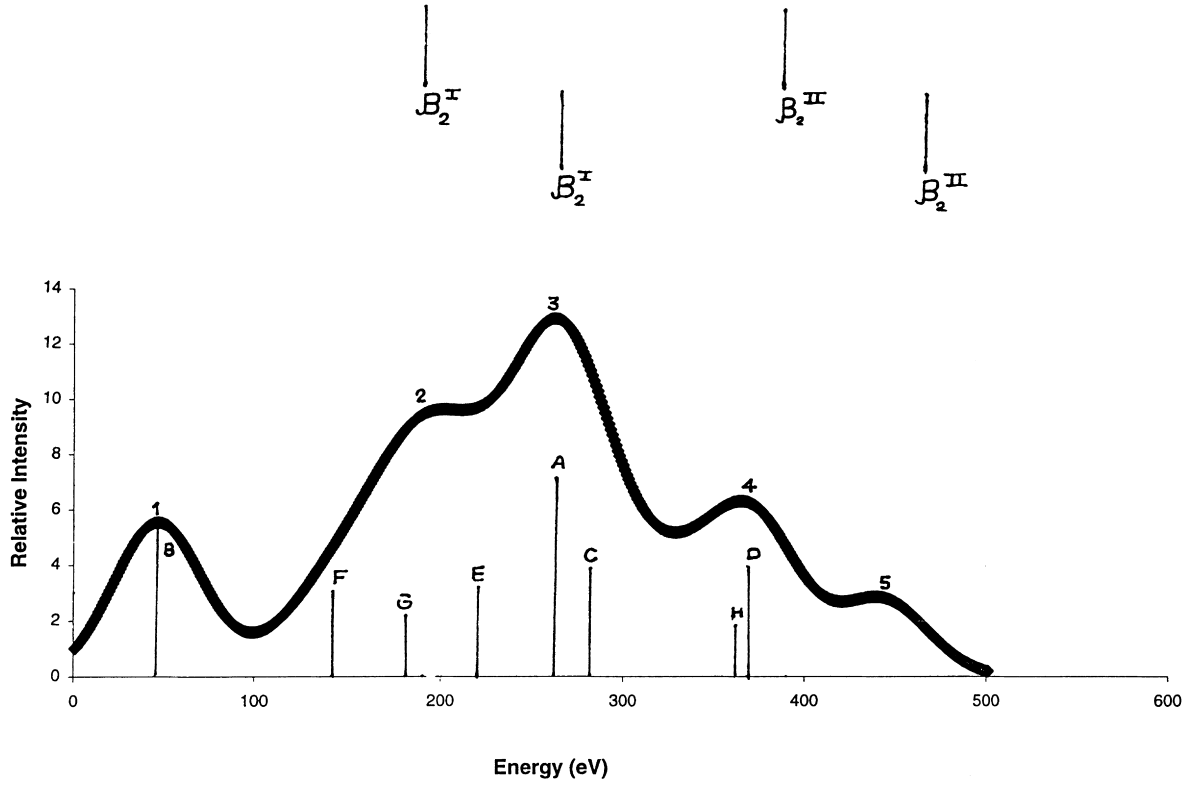

Fig. 2. The computed L_3M_x–$M_xN_{4,5}$ spectrum of $_{76}$Os. For bars at the top, see the caption to Fig. 1.

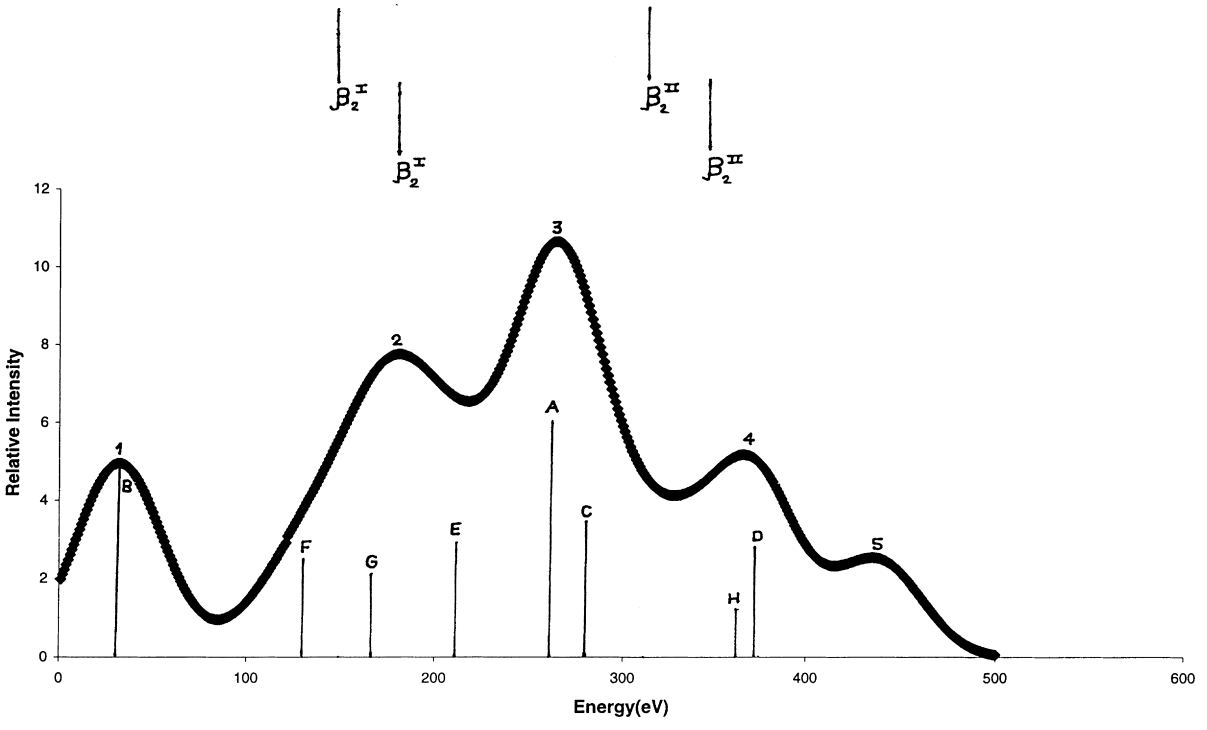

Fig. 3. The computed L_3M_x–$M_xN_{4,5}$ spectrum of $_{78}$Pt. For bars at the top, see the caption to Fig. 1.

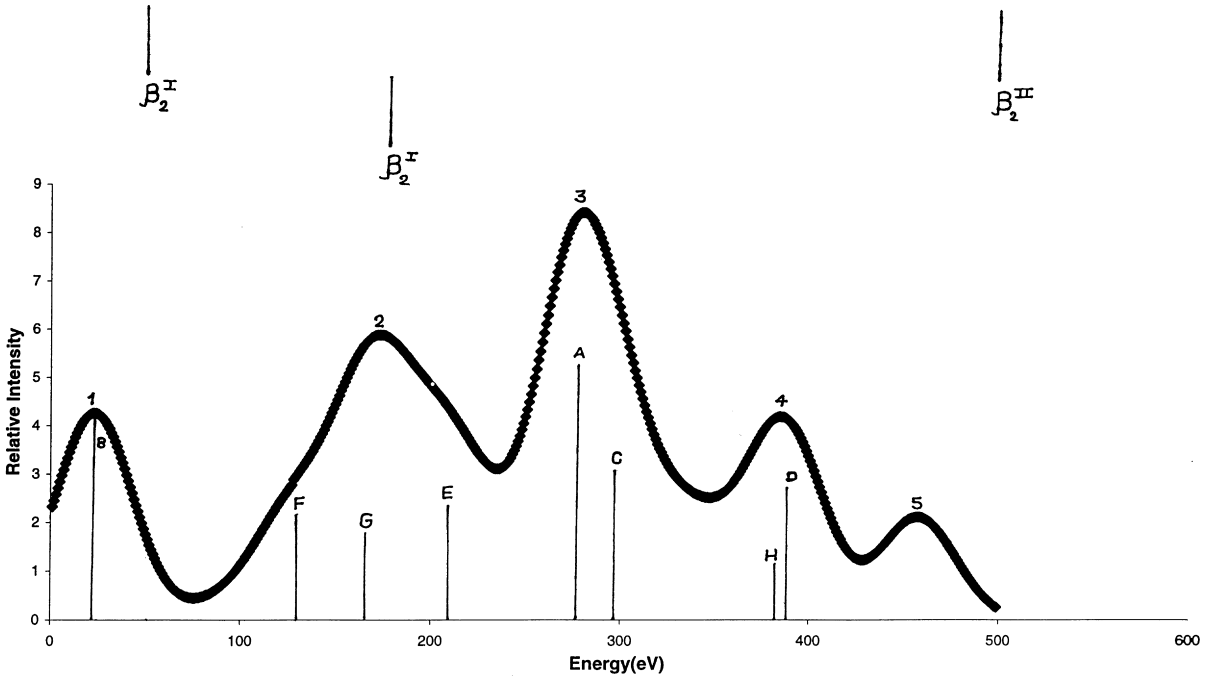

Fig. 4. The computed L_3M_x–$M_xN_{4,5}$ spectrum of $_{80}$Hg. For bars at the top, see the caption to Fig. 1.

seen by the values in the last columns of Tables 2–4. The measured spectra are also presented in Figs. 1–7, in each of which the measured satellite data are shown by vertical bars in two rows at the top of the figure. In the upper row, the measured [1] satellite positions are shown while in the lower row, the measured data have been shown after shifting them horizontally by the average of the discrepancies in measured and computed

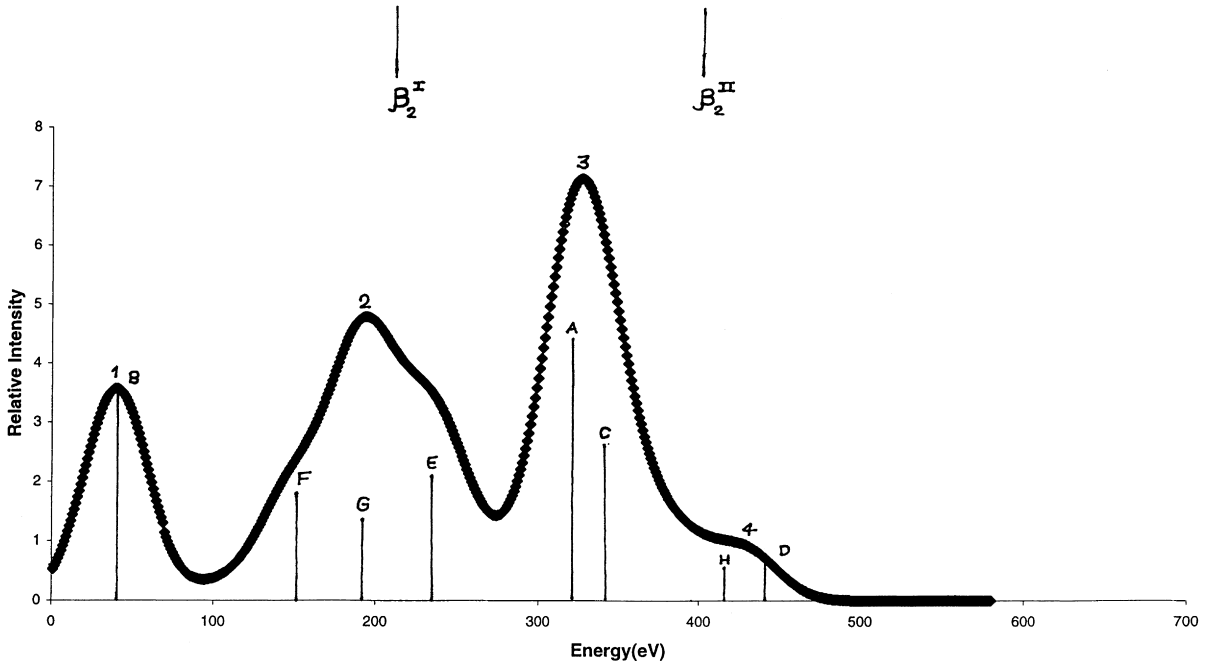

Fig. 5. The computed L_3M_x–$M_xN_{4,5}$ spectrum of $_{82}$Pb. For bars at the top, see the caption to Fig. 1.

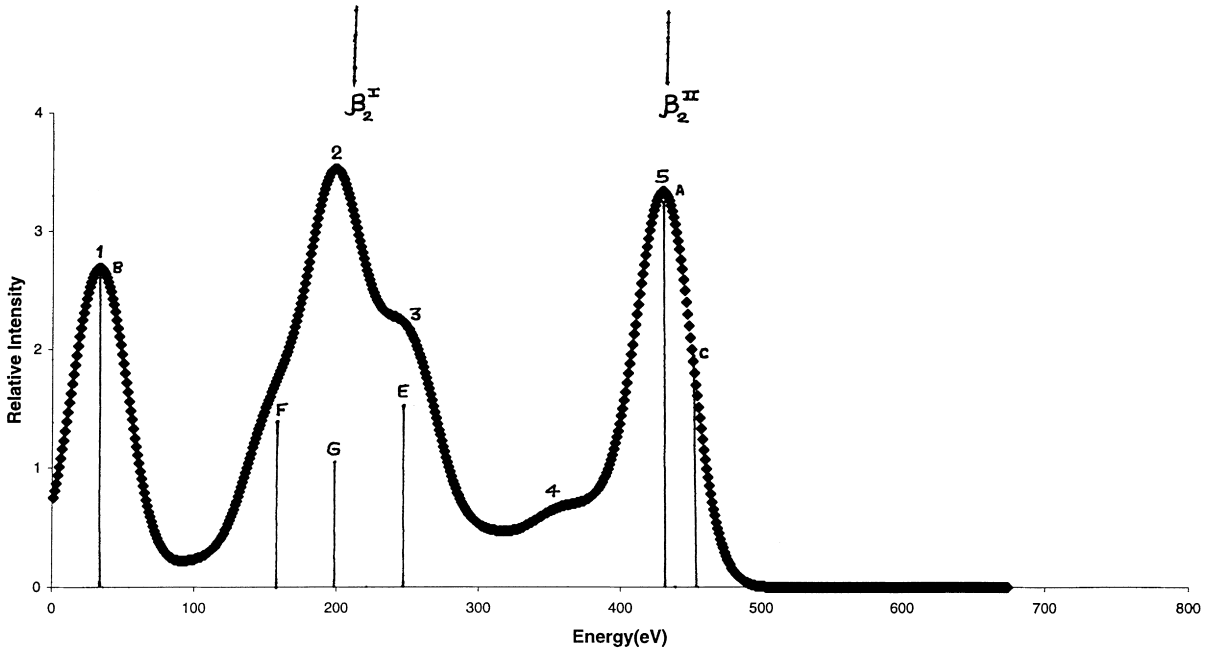

Fig. 6. The computed L_3M_x–$M_xN_{4,5}$ spectrum of $_{88}$Ra. For bars at the top, see the caption to Fig. 1.

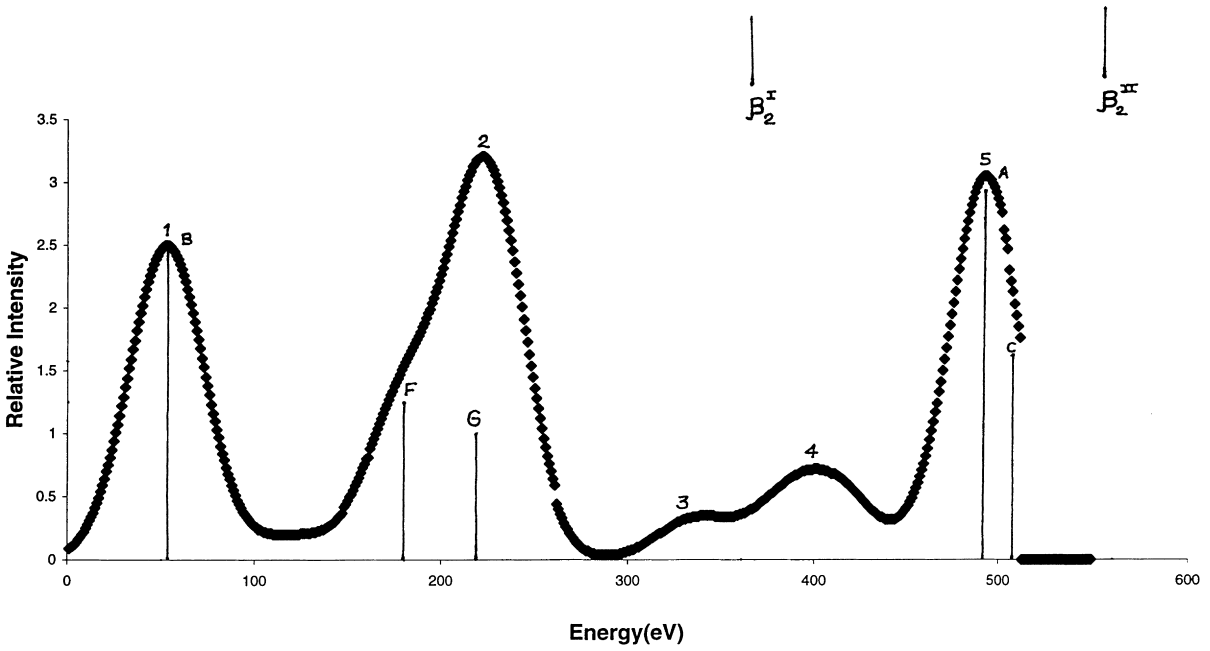

Fig. 7. The computed L_3M_x–$M_xN_{4,5}$ spectrum of $_{90}$Th. For bars at the top, see the caption to Fig. 1.

Table 1
The intense transitions of L_3M_x–$M_xN_{4,5}$ ($x = 1$–5) array, with their names as used in the text. Their relative intensities are also presented. In $_{74}$W, $_{80}$Hg and $_{90}$Th, both the Coster Kronig transitions and shake-off probabilities have been added

S. no.	Transition[a]	Symbol of the transition used in the text	Rel. int. $Z = 74$	Rel. int. $Z = 80$	Rel. int. $Z = 90$
1	$^3F_4$–$^3G_5$ (3d)	A	7.57	5.21	3.05
2	$^3F_4$–$^3F_4$ (3d)	B	6.19	4.26	2.50
3	$^3F_4$–$^3D_3$ (3d)	C	4.42	3.04	1.78
4	$^1F_3$–$^1G_4$ (3d)	D	3.98	2.74	1.60
5	$^3D_3$–$^3F_4$ (3d)	E	3.48	2.39	1.40
6	$^1D_2$–$^1F_3$ (3d)	F	3.09	2.13	1.25
7	$^3D_2$–$^3F_3$ (3d)	G	2.40	1.65	0.97
8	$^3P_0$–$^3D_1$ (3d)	H	1.35	0.93	0.54
9	$^3D_3$–$^3D_3$ (3d)		3.54	2.43	1.43
10	$^3P_1$–$^3D_2$ (3d)		3.06	2.10	1.23
11	$^1F_3$–$^1D_2$ (3d)		2.21	1.52	0.89
12	$^1P_1$–$^1D_2$ (3d)		2.21	1.52	0.89
13	$^3D_3$–$^3P_2$ (3d)		1.72	1.18	0.69
14	$^1D_2$–$^1P_1$ (3d)		1.32	0.91	0.53

[a] The spectator hole position has been shown in the braces along with the transitions.

peak energies. The transition assignments to the satellites based on the identification of the peaks are discussed below.

3.1. $L_3M_{4,5}$–$M_{4,5}N_{4,5}$ array

3.1.1. The transitions A, C and E

Out of the three most intense transitions, A, C and E, of the complete L_3M_x–$M_xN_{4,5}$ array, A and C have energies very close to each other in all the elements $_{74}$W to $_{90}$Th. Their superposition gives rise to the highest peak in each of the spectra, marked no. 2 in $_{74}$W and $_{88}$Ra to $_{90}$Th (Figs. 1, 6 and 7) and marked no. 3 in the spectra of $Z = 76$–82 (Figs. 2–5). This is, hereby, identified as the satellite β_2^{I} in the spectra of $_{74}$W and $_{76}$Os, and in the spectra of $Z = 78$–90 is identified as the line β_2^{II}. The transition E has intensity nearly one-third of A and has energy close to it and on its higher side. It also contributes in forming peak nos. 2 and 3 in the above elements and, hence, can be taken as the supporting origin for the line β_2^{I} in the spectra of $Z = 74$ to 76 and β_2^{II} in the spectra of $Z = {}_{78}$Pt to $_{90}$Th.

3.1.2. The transitions E, F and G

The transitions E, F and G of the $L_3M_{4,5}$–$M_{4,5}N_{4,5}$ array all contribute to peak no. 2 (Figs. 3–7). This is, hereby, identified as the satellite β_2^{I} in the spectra of the elements $Z = {}_{78}$Pt to $_{90}$Th. It can be noted that this peak merges with peak no. 2 in $_{74}$W and gives rise to a shoulder in $_{76}$Os on the lower energy tail of peak no. 3.

3.1.3. The transitions D and H

The transition D has the highest energy of all eight transitions A–H of the array being considered in the present study. The peak formed by it has been marked no. 3 in $_{74}$W and no. 4 in $_{76}$Os (Figs. 1 and 2). This is, hereby, identified as the satellite β_2^{II} in the spectra of $Z = 74$–76. The transition H has an intensity nearly half of D and has energy close to it on its higher side. Hence, it can be taken as the supporting origin for the line β_2^{II}.

3.1.4. The transition B

The second most intense transition in the array $L_3M_{4,5}$–$M_{4,5}N_{4,5}$ considered presently is $^3F_4$–$^3F_4$, named B in Table 1. It gives rise to a well-separated peak, marked no. 1, in each of the calculated spectra presented in Figs. 1–7. This peak merges with the $L\beta_{2,15}$ line in all these spectra and, hence, is not observed independently.

Table 5
The $L\beta_2$ satellites and corresponding L_3M_x–$M_xN_{4,5}$ transitions in elements $_{74}$W to $_{90}$Th

S. no.	Satellites	Transitions						
		Z						
		74	76	78	80	82	88	90
1	β_2^{I}	A,C,E	A,C,E	E,F,G	E,F,G	E,F,G	E,F,G	E,F,G
2	β_2^{II}	D,H	D,H	A,C	A,C	A,C	A,C	A,C

Table 2
The calculated energy and height of peak nos. 2 and 3, and of the transitions A, C and E, which give rise to these peaks. The corresponding measured β_2^I and β_2^{II} energies are also shown

S. no.	Z	A		C		E		Computed peak data		Measured β_2^I and β_2^{II} energies (eV)	Difference between calculated and measured spectra
		Energy (eV)	Rel. int.	Energy (eV)	Rel. int.	Energy (eV)	Rel. int.	Energy (eV)	Rel. int.		
1	74	10022.4	7.57	10024.0	4.42	10020.8	3.48	10022.2	18.32	10008.2 β_2^I	14.0
2	76	10661.0	6.77	10662.7	3.95	10656.8	3.11	10661.3	12.91	10654.0 β_2^I	7.3
3	78	11316.0	6.05	11317.8	3.53	–	–	11316.7	10.66	11321.0 β_2^{II}	–
4	80	11992.5	5.21	11994.4	3.04	–	–	11993.3	8.41	12015.0 β_2^{II}	–
5	82	12692.0	4.36	12694.0	2.55	–	–	12692.9	7.14	12699.7 β_2^{II}	–
6	88	14928.0	3.30	14930.2	1.92	–	–	14928.0	3.34	14929.5 β_2^{II}	–
7	90	15704.3	3.05	15706.7	1.78	–	–	15704.3	3.05	15711.0 β_2^{II}	–

Table 3
The calculated energy and height of transitions E–G and of corresponding peak no. 2. The satellites β_2^I to which this peak is identified are also shown

S. no.	Z	E		F		G		Computed peak data		Measured β_2^I energies (eV)	Difference between calculated and measured spectra
		Energy (eV)	Rel. int.	Energy (eV)	Rel. int.	Energy (eV)	Rel. int.	Energy (eV)	Rel. int.		
1	74	10020.8	3.48	10013.5	3.09	10017.0	2.40	[a]	[a]	–	–
2	76	10656.8	3.11	10649.2	2.76	10652.7	2.14	[a]	[a]	–	–
3	78	11310.9	2.78	11303.1	2.47	11306.6	1.92	11308.3	7.76	11305.0	3.3
4	80	11985.8	2.39	11977.7	2.13	11981.4	1.65	11982.6	5.88	11970.0	12.6
5	82	12683.2	2.00	12674.9	1.78	12678.7	1.38	12679.6	4.79	12681.9	–
6	88	14909.4	1.51	14900.4	1.34	14904.5	1.04	14904.9	3.53	14907.2	–
7	90	–	–	15673.0	1.25	15677.1	0.97	15677.2	3.21	15691.0	–

[a] This transitions merges with A and C to form peak no.2.

Table 4
The calculated energy and height of transitions D and H and of computed peak nos. 3 and 4. The satellites β_2^{II} to which this peak is identified are also shown

S. no.	Z	D		H		Computed peak data		Measured β_2^{II} energies (eV)	Difference between calculated and measured spectra (eV)
		Energy (eV)	Rel. int.	Energy (eV)	Rel. int.	Energy (eV)	Rel. int.		
1	74	10033.3	3.98	10032.3	1.35	10032.8	7.99	10033.0 β_2^{II}	–
2	76	10672.2	3.55	10671.3	1.21	10671.6	6.30	10674.0 β_2^{II}	–
3	78	11327.5	3.17	11325.7	1.08	11326.7	5.18	–	–
4	80	12004.1	2.74	12002.7	0.93	12003.6	4.19	–	–
5	82	12703.9	2.29	12703.1	0.78	12701.2	1.05	–	–
6	88	14940.2	1.73	14939.7	0.59	–	–	–	–
7	90	15716.8	1.60	15716.4	0.54	–	–	–	–

3.2. Other transitions

The transitions shown at s. nos. 9–14 in Table 1 have energies lying in the range of the above-mentioned transitions, A–H and, therefore, merge with one of the peaks formed by them. Transition nos. 9 and 10, namely $^3D_3-^3D_3$ and $^3P_1-^3D_2$ of the $L_3M_{4,5}-M_{4,5}N_{4,5}$ array are very weak. They give rise to a separate peak, marked no. 4 in $_{74}$W and no. 5 in $_{76}$Os to $_{80}$Hg in Figs. 1–4. However, no line has been observed corresponding to this peak.

4. Conclusion

The present study has revealed that two satellites β_2^I and β_2^{II} observed in the $L\beta_2$ spectra of elements $Z = 74$–90, with a few exceptions, arise mainly due to the $L_3-N_{4,5}$ transitions in the presence of an M-shell spectator vacancy. The association of various intense transitions of the array with the measured satellite is presented in Table 5. On the basis of the agreement between computed spectra and measured satellites, it is observed that the satellite β_2^I is emitted by the superposition of two transitions, $^3F_4-^3G_5$ and $^3F_4-^3D_3$ in the spectra of elements with $Z = 74$–76 and β_2^{II} in the spectra of elements with $Z = {}_{78}$Pt to $_{90}$Th, while in the range of elements with $Z = 78$ to 90, β_2^I has been assigned to the transitions $^3D_3-^3F_4$ and $^1D_2-^1F_3$. It has been well established that the transition $^1F_3-^1G_4$ is the main source of the emission of the satellite β_2^{II} in the elements $Z = 74$–76. Unfortunately, no experimental data are available on these intensities.

References

[1] Y. Cauchois, C. Senemaud, X-ray Wavelength Tables, 2nd ed., Pergamon Press, Oxford, 1978.
[2] S.N. Soni, M.H. Massoud, J. Phys. Chem. Solids 58 (1) (1996) 145–151.
[3] S.N. Soni, S. Poonia, J. Phys. Chem. Solids 61 (9) (2000) 1509–1518.
[4] E.U. Condon, C.H. Shortley, The Theory of Atomic Spectra, Cambridge University Press, Cambridge, 1967 (pp. 241–243).
[5] J.A. Bearden, A.F. Burr, Rev. Mod. Phys. 39 (1967) 78–127.
[6] F.P. Larkins, At. Data Nucl. Data Tables 20 (1977) 311–387.
[7] D.L. Moores, L.B. Golden, D.H. Sampson, J. Phys. B 13 (1980) 385–395.
[8] E.J. McGuire, L-shell Auger, CK and radiative matrix elements, Sandia Laboratories Report no. SC-RR-710075, 1971.
[9] T.A. Carlson, C.W. Nestor Jr., Phys. Rev. A 8 (6) (1972) 2887–2894.
[10] S.N. Soni, J. Phys. Chem. Solids 45 (1984) 797–803.
[11] S.N. Soni, J. Phys. B: At. Mol. Opt. Phys. 23 (1990) 1117–1128.
[12] N. Maskil, M. Deutsch, Phys. Rev. A 38 (7) (1988) 3467–3472.